

2014

Estimation of crop gross primary production (GPP): fAPAR_{chl} versus MOD15A2 FPAR

Qingyuan Zhang
NASA, Greenbelt, MD, qyz72@yahoo.com

Yen-Ben Cheng
NASA, Greenbelt, MD


A. I. Lyapustin
NASA Goddard Space Flight Center

Yujie Wang
NASA, Greenbelt, MD

Feng Gao
USDA-ARS, Beltsville, MD, Feng.Gao@ars.usda.gov

See next page for additional authors

Follow this and additional works at: <http://digitalcommons.unl.edu/natrespapers>

 Part of the [Atmospheric Sciences Commons](#), [Environmental Indicators and Impact Assessment Commons](#), [Environmental Monitoring Commons](#), [Instrumentation Commons](#), [Other Earth Sciences Commons](#), [Other Environmental Sciences Commons](#), and the [Systems Engineering and Multidisciplinary Design Optimization Commons](#)

Zhang, Qingyuan; Cheng, Yen-Ben; Lyapustin, A. I.; Wang, Yujie; Gao, Feng; Suyker, Andrew E.; Verma, Shashi B.; and Middleton, Elizabeth M., "Estimation of crop gross primary production (GPP): fAPAR_{chl} versus MOD15A2 FPAR" (2014). *Papers in Natural Resources*. 465.
<http://digitalcommons.unl.edu/natrespapers/465>

This Article is brought to you for free and open access by the Natural Resources, School of at DigitalCommons@University of Nebraska - Lincoln. It has been accepted for inclusion in Papers in Natural Resources by an authorized administrator of DigitalCommons@University of Nebraska - Lincoln.

Authors

Qingyuan Zhang, Yen-Ben Cheng, A. I. Lyapustin, Yujie Wang, Feng Gao, Andrew E. Suyker, Shashi B. Verma, and Elizabeth M. Middleton



Estimation of crop gross primary production (GPP): fAPAR_{chl} versus MOD15A2 FPAR



Qingyuan Zhang^{a,b,*}, Yen-Ben Cheng^{c,b}, Alexei I. Lyapustin^d, Yujie Wang^{e,b}, Feng Gao^f, Andrew Suyker^g, Shashi Verma^g, Elizabeth M. Middleton^b

^a Universities Space Research Association, Columbia, MD 21044, USA

^b Biospheric Sciences Laboratory, National Aeronautics and Space Administration/Goddard Space Flight Center, Greenbelt, MD 20771, USA

^c Sigma Space Corporation, Lanham, MD 20706, USA

^d Climate and Radiation Laboratory, Code 613, National Aeronautics and Space Administration Goddard Space Flight Center, Greenbelt, MD 20771, USA

^e Goddard Earth Sciences and Technology Center, University of Maryland Baltimore County, Baltimore, MD 21228, USA

^f Hydrology and Remote Sensing Laboratory, Agricultural Research Service, US Department of Agriculture, Beltsville, MD 20705, USA

^g School of Natural Resources, University of Nebraska—Lincoln, Lincoln, NE 68588, USA

ARTICLE INFO

Article history:

Received 27 January 2014

Received in revised form 12 July 2014

Accepted 16 July 2014

Available online 14 August 2014

Keywords:

GPP

MODIS

MOD15A2 FPAR

fAPAR_{chl}

ABSTRACT

Photosynthesis (PSN) is a pigment level process in which antenna pigments (predominately chlorophylls) in chloroplasts absorb photosynthetically active radiation (PAR) for the photochemical process. PAR absorbed by foliar non-photosynthetic components is not used for PSN. The fraction of PAR absorbed (fAPAR) by a canopy/vegetation (i.e., fAPAR_{canopy}) derived from the Moderate Resolution Imaging Spectroradiometer (MODIS) images, referred to as MOD15A2 FPAR, has been used to compute absorbed PAR (APAR) for PSN (APAR_{PSN}) which is utilized to produce the standard MODIS gross primary production (GPP) product, referred to as MOD17A2 GPP. In this study, the fraction of PAR absorbed by chlorophyll throughout the canopy (fAPAR_{chl}) was retrieved from MODIS images for three AmeriFlux crop fields in Nebraska. There are few studies in the literature that compare the performance of MOD15A2 FPAR versus fAPAR_{chl} in GPP estimation. In our study MOD15A2 FPAR and the retrieved fAPAR_{chl} were compared with field fAPAR_{canopy} and the fraction of PAR absorbed by green leaves of the vegetation (fAPAR_{green}). MOD15A2 FPAR overestimated field fAPAR_{canopy} in spring and in fall, and underestimated field fAPAR_{canopy} in midsummer whereas fAPAR_{chl} correctly captured the seasonal phenology. The retrieved fAPAR_{chl} agreed well with field fAPAR_{green} at early crop growth stage in June, and was less than field fAPAR_{green} in late July, August and September. GPP estimates with fAPAR_{chl} and with MOD15A2 FPAR were compared to tower flux GPP. GPP simulated with fAPAR_{chl} was corroborated with tower flux GPP. Improvements in crop GPP estimation were achieved by replacing MOD15A2 FPAR with fAPAR_{chl} which also reduced uncertainties of crop GPP estimates by 1.12–2.37 g C m⁻² d⁻¹.

© 2014 Elsevier Inc. All rights reserved.

1. Introduction

Terrestrial vegetation captures carbon as carbon dioxide (CO₂) and simultaneously releases O₂ and diffuses water (H₂O) through the process of photosynthesis (PSN). PSN is a basic physiological function of vegetation that relies on energy absorbed by chlorophyll (chl) for plant growth and biomass accumulation (Emmanuel, Killough, Post, & Shugart, 1984). The Earth Observing System (EOS) has been designed to capture the patterns of the Earth's terrestrial ecosystems, including estimates of photosynthetic activity, through linking remote sensing observations to models (Ustin et al., 1991). The FOREST-BGC (BioGeoChemical cycles)

model is a process model that depicts the cycles of carbon, water and nitrogen through forest ecosystems, including the vegetation photosynthesis process which uses leaf area index (LAI) as one of the variable inputs (Running, 1984; Running & Coughlan, 1988; Running & Gower, 1991). The theoretical studies by Sellers (1985, 1987) suggested that the normalized difference vegetation index (NDVI) (Deering, 1978; Tucker, 1979) of the advanced very high resolution radiometer (AVHRR) is directly related to PSN and vegetation transpiration, especially for vegetation experiencing optimal temperature and water availability. Monteith (1972, 1977) suggested crop GPP could be estimated as $GPP = \epsilon \times fAPAR_{PSN} \times PAR$, where PAR is photosynthetically active radiation, fAPAR_{PSN} is the fraction of PAR absorbed for PSN, and ϵ is photosynthetic light use efficiency (LUE). A pre-launch algorithm was developed in 1997 (Myneni, Nemani, & Running, 1997) to estimate LAI and the fraction of PAR absorbed (fAPAR) by a canopy/vegetation (fAPAR_{canopy}, also called FPAR) using NDVI for the moderate resolution

* Corresponding author at: Building 33, Room G321, Biospheric Sciences Laboratory, Code 618, NASA/Goddard Space Flight Center, Greenbelt, MD 20771, USA. Tel.: +1 301 614 6672.

E-mail address: qyz72@yahoo.com (Q. Zhang).

imaging spectroradiometer (MODIS), and is used as a backup for the standard MODIS LAI/FPAR (MOD15A2 LAI/FPAR) product when the retrieval based on the radiative transfer modeling fails (Knyazikhin, Martonchik, Myneni, Diner, & Running, 1998; Myneni et al., 2002). The BIOME-BGC model developed from FOREST-BGC has been used to produce the MODIS GPP standard product (MOD17A2 GPP) which integrated the understanding and knowledge at that time including the NDVI-LAI-FPAR linkage. The MOD15A2 FPAR product and a biome parameter look up table (BPLUT) of ϵ are two of the inputs used to produce MOD17A2 GPP (Justice et al., 1998; Running, Thornton, Nemani, & Glassy, 2000; Running et al., 2004; Zhao & Running, 2010).

Zhang et al. have made efforts to retrieve the fraction of PAR absorbed by chlorophyll throughout the canopy ($fAPAR_{chl}$) using a coupled canopy-leaf radiative transfer model and surface reflectance of MODIS bands 1–7, obtained from actual MODIS satellite data and from MODIS-like data synthesized at 30 m or 60 m from EO-1 Hyperion images (Zhang, 2003; Zhang, Middleton, Cheng, & Landis, 2013; Zhang, Middleton, Gao, & Cheng, 2012; Zhang et al., 2005, 2009). The inverse algorithm can also retrieve fAPAR of foliage ($fAPAR_{foliage}$), fAPAR of foliage non-chlorophyll components ($fAPAR_{non-chl}$), LAI, and the photosynthetic section (chlorophyll) of LAI (LAI_{chl}). Zhang et al. (2013) showed that (1) $fAPAR_{canopy} \neq fAPAR_{chl}$; and (2) both $fAPAR_{chl}$ and $fAPAR_{non-chl}$ of deciduous broadleaf forests and coniferous needleleaf forests varied seasonally.

Photosynthesis is a pigment level process in which antenna pigments (predominately chlorophylls) in chloroplasts absorb solar radiation for the photochemical process. Therefore estimating GPP with $fAPAR_{chl}$ is more consistent with the photosynthetic process than MOD15A2 FPAR. However, few studies have compared the performance of these two algorithms in GPP estimation. The objectives of this study succinctly are: (1) to evaluate the retrievals of $fAPAR_{chl}$ and MOD15A2 FPAR through comparison with crop field measurements, and (2) to evaluate the GPP estimation performance through comparison with tower flux GPP.

2. Methods

2.1. Study fields and field measured fAPARs

We selected three AmeriFlux crop fields for this study which are located at the University of Nebraska–Lincoln (UNL) Agricultural Research and Development Center near Mead, Nebraska (US-NE1, US-NE2 and US-NE3). The US-NE1 site (41°09′54.2″N, 96°28′35.9″W) and US-NE2 site (41°09′53.6″N, 96°28′07.5″W) are two circular fields (radius ~390 m) and the US-NE3 site (41°10′46.7″N, 96°26′22.4″W) is a square field (length ~790 m). The US-NE1 field is a continuous maize (*Zea mays* L.) field while the US-NE2 and US-NE3 fields are maize-soybean (*Glycine max* [L.] Merr.) rotation fields (maize is planted in odd years). The US-NE1 and US-NE2 fields are equipped with center-pivot irrigation systems while the US-NE3 field entirely relies on rainfall (Gitelson, Viña, J.G.M., Verma, & Suyker, 2008; Peng, Gitelson, & Sakamoto, 2013). Soybean is a C3 crop and maize is a C4 crop. These sites provide an opportunity to examine the GPP estimation performance using MOD15A2 FPAR versus $fAPAR_{chl}$ for different vegetation types (C3 vs. C4 crops) in both irrigated and non-irrigated ecosystems.

Field activities were conducted to determine $fAPAR_{canopy}$ and $fAPAR$ by green leaves of the canopy ($fAPAR_{green}$) (Peng, Gitelson, Keydan, Rundquist, & Moses, 2011). The $fAPAR_{green}$ is defined as:

$$fAPAR_{green} = fAPAR_{canopy} \times \frac{LAI_{green}}{LAI} \quad (1)$$

where LAI_{green} is green LAI (Peng et al., 2011). The point quantum sensors (LI-190, LI-COR Inc., Lincoln, NE) were used to measure incoming PAR from the atmosphere, PAR reflected out of the canopy by the

canopy and soil/background, PAR transmitted through the canopy, and PAR reflected into the canopy from soil. All of these PARs were used to compute absorbed PAR (APAR) by the canopy ($APAR_{canopy}$) and $fAPAR_{canopy}$ [see (Peng et al., 2011) for details]. Each sampled plant was separated into green leaves, dead leaves and litter components, and both green and dead leaves were run through the same area meter (Model LI-3100, Li-Cor, Inc., Lincoln NE). These leaf area measurements were used to determine (total) LAI and LAI_{green} (Gitelson et al., 2003), from which $fAPAR_{green}$ was computed with Eq. (1). The field $fAPAR_{canopy}$, $fAPAR_{green}$, LAI and LAI_{green} were provided by Drs. Gitelson and Peng from UNL, and were used to evaluate both MOD15A2 LAI/FPAR and our $fAPAR_{chl}/LAI_{chl}$ retrievals (see definition of LAI_{chl} in Eq. (4)).

Each crop field is equipped with an eddy covariance flux tower. Science quality algorithms have been applied to process tower measurements. The level 2 gap filled tower PAR and GPP data is publicly available and can be downloaded from <ftp://cdiac.ornl.gov/pub/ameriflux/data/>. The nighttime ecosystem respiration/temperature Q_{10} relationship was used to estimate the daytime ecosystem respiration. Daily GPP was computed by subtracting respiration (R) from net ecosystem exchange (NEE), i.e., $GPP = NEE - R$ (Suyker, Verma, Burba, & Arkebauer, 2005). The GPP estimates obtained with MOD15A2 FPAR and $fAPAR_{chl}$ algorithms were compared to tower flux GPP, as described below.

2.2. MODIS retrieved fAPARs: MOD15A2 FPAR and $fAPAR_{chl}$

The MOD15A2 FPAR product is a standard 1 km 8-day $fAPAR_{canopy}$ product for EOS-MODIS (Myneni et al., 2002). MOD15A2 FPAR of the three NE crop fields can be freely downloaded from the Oak Ridge National Laboratory (<http://daac.ornl.gov/MODIS/>).

A procedure to produce an 8-day MODIS $fAPAR_{chl}$ product has recently been developed (Zhang, Cheng, Lyapustin, Wang, Xiao, et al., 2014; Zhang, Cheng, Lyapustin, Wang, Zhang, et al., 2014). MODIS land bands (1–7) have variable nadir spatial resolutions between 250 and 500 m: B1 (red, 620–670 nm), B2 (near infrared, NIR₁, 841–876 nm), B3 (blue, 459–479 nm), B4 (green, 545–565 nm), B5 (NIR₂, 1230–1250 nm), B6 (shortwave infrared, SWIR₁, 1628–1652 nm) and B7 (SWIR₂, 2105–2155 nm). MODIS L1B calibrated radiance data (MOD021KM and MOD02HKM) and geolocation data (MOD03) were downloaded from <https://ladsweb.nascom.nasa.gov:9400/data/>. The centers of the original 500 m grids defined in the standard MOD09 reflectance products (Wolfe, Roy, & Vermote, 1998) that encompass the three tower sites are not the centers of the fields [please check Fig. 2 in (Guindin-Garcia, Gitelson, Arkebauer, Shanahan, & Weiss, 2012) for details]. A modified gridding approach was used in this study (Zhang, Cheng, Lyapustin, Wang, Xiao, et al., 2014). We defined the centers of the three fields as centers of three 500 m grids. The L1B radiance data from each swath were then gridded at 500 m resolution for MODIS bands 1–7 with area weights of each MODIS observation. The gridded observations were then atmospherically corrected with the Multi-Angle Implementation of Atmospheric Correction (MAIAC) algorithm (Lyapustin, Martonchik, Wang, Laszlo, & Korkin, 2011a; Lyapustin, Wang, & Frey, 2008; Lyapustin et al., 2011b, 2012). The bidirectional reflectance factors (BRF, also called surface reflectance) derived with MAIAC were used in the algorithm we developed to retrieve $fAPAR_{chl}$ (Zhang, Cheng, Lyapustin, Wang, Zhang, et al., 2014; Zhang et al., 2005, 2009, 2012, 2013). Only the MODIS observations with view zenith angles (VZA) less than 35° were used in the retrieval algorithm to reduce the observation footprint impact (Zhang, Cheng, Lyapustin, Wang, Xiao, et al., 2014).

Here is a brief description of the retrieval algorithm. We use the PROSAIL2 model, a coupled canopy-leaf radiative transfer model (Zhang et al., 2005, 2009, 2012, 2013). The foliage component of a canopy is partitioned into chl and non-chlorophyll (non-chl) components, where non-chl is composed of non-photosynthetic pigments (referred

to as brown pigment) and dry matter. The $fAPAR_{non-chl}$, $fAPAR_{foliage}$ and LAI_{chl} can be computed as:

$$fAPAR_{non-chl} = fAPAR_{brown_pigment} + fAPAR_{dry_matter} \quad (2)$$

$$fAPAR_{foliage} = fAPAR_{chl} + fAPAR_{non-chl} \quad (3)$$

$$LAI_{chl} = LAI * \frac{fAPAR_{chl}}{fAPAR_{foliage}} \quad (4)$$

We employ the Metropolis algorithm (Metropolis, Rosenbluth, Rosenbluth, Teller, & Teller, 1953), a type of Markov Chain Monte Carlo (MCMC) estimation procedure (Gelman, Carlin, Stern, & Rubin, 2000), to invert the PROSAIL2 model to retrieve biophysical and biochemical variables of PROSAIL2. This method estimates posterior probability distributions per variable. The posterior statistical distributions provide the mode (i.e., best point solution) values per variable. The $fAPARs$ ($fAPAR_{foliage}$, $fAPAR_{chl}$, $fAPAR_{non-chl}$) and LAI_{chl} are then computed with the estimated model variables through PROSAIL2 forward simulations.

To be comparable to MOD15A2 FPAR/LAI, $fAPAR_{chl}/LAI_{chl}$ retrievals for every 8-day period started from the first day of year (DOY) in each year, and were averaged to represent the 8-day values.

2.3. MODIS retrieved $fAPARs/LAIs$ versus field measured $fAPARs/LAIs$

Both MOD15A2 FPAR/LAI and $fAPAR_{chl}/LAI_{chl}$ were derived using MODIS surface reflectance. The $fAPAR_{green}$ was computed with the field values for $fAPAR_{canopy}$, LAI and LAI_{green} . Both the field $fAPAR_{canopy}$ and MOD15A2 FPAR product are defined as FPAR at canopy level. In concept, for a given field at a given time, neither $fAPAR_{chl}$ nor $fAPAR_{green}$ should be greater than FPAR at canopy level, and neither LAI_{chl} nor LAI_{green} should be greater than (total) LAI.

The time series of the retrieved MODIS $fAPARs$ (MOD15A2 FPAR and $fAPAR_{chl}$) and field $fAPARs$ (field $fAPAR_{canopy}$ and $fAPAR_{green}$) during 2001–2004 were plotted to compare to each other. The time series of the retrieved MODIS LAIs (MOD15A2 LAI and LAI_{chl}) and field LAIs (field LAI and LAI_{green}) during 2001–2004 were also plotted to compare to each other. Analysis and evaluation were carried out (see Sections 3 and 4).

2.4. GPP estimation performance: MOD15A2 FPAR versus $fAPAR_{chl}$

Tower measured PAR was averaged every 8-day to match the temporal interval of the MOD15A2 FPAR product. In order to evaluate the GPP estimation performance using the MODIS retrieved $fAPARs$, the products of the retrieved $fAPARs$ and 8-day mean daily PAR (MOD15A2 FPAR \times PAR and $fAPAR_{chl} \times$ PAR) were compared against the tower flux 8-day mean daily GPP, respectively. We tested the simple linear model: $y = ax$, where $y = GPP$; x is APAR of canopy or of chlorophyll ($APAR_{canopy}$ or $APAR_{chl}$), i.e., $x = fAPAR_x \times PAR$ ($fAPAR_x = MOD15A2$ FPAR or $fAPAR_{chl}$); and the coefficient “a” was computed with the least squares best fit algorithm. Statistics for the coefficient of determination (R^2) and the root mean square error (RMSE) are reported to evaluate model performance.

3. Results

Fig. 1 shows the intensive field measurements at the US-NE1 field from June to September during 2001–2004. Seasonal dynamics of field $fAPAR_{canopy}$, $fAPAR_{green}$, LAI and LAI_{green} , and seasonal dynamics of MOD15A2 FPAR/LAI and the $fAPAR_{chl}/LAI_{chl}$ retrievals are presented. The $fAPAR_{chl}$ and LAI_{chl} retrievals were much lower than the counterpart MOD15A2 FPAR and LAI values during the spring seasons before new leaves emerged. The $fAPAR_{chl}$ retrievals were also much lower

than the counterpart MOD15A2 FPAR values during the senescent stage and after harvesting. The difference between MOD15A2 FPAR and field $fAPAR_{canopy}$ was >0.17 during June to September. The difference between MOD15A2 LAI and field LAI was >2.4 during peak of the growing season. Field $fAPAR_{green}$ matched well with the $fAPAR_{chl}$ retrievals during the early vegetative stage in June and early July but was higher than $fAPAR_{chl}$ during the mature/reproductive and senescent stages in late July, August and September. In addition, similar patterns were observed between LAI_{green} and LAI_{chl} . In order to save pages, we do not exhibit the similar figures for US-NE2 and US-NE3 here.

The product of $fAPAR_x$ (MOD15A2 FPAR or $fAPAR_{chl}$) and PAR for each crop type per field was compared against tower flux GPP to determine the function for the simple linear regression model. The function $y = ax$, R^2 and RMSE were listed in Table 1, where the dependent variable (y) is tower flux GPP, and the independent variable (x) is the product of PAR and $fAPAR_x$. The physiological meaning of slope “a” is average light use efficiency (LUE): it means LUE at canopy level ($LUE_{canopy} = \frac{GPP}{MOD15A2\ FPAR \times PAR}$) for MOD15A2 FPAR and means LUE at chlorophyll level ($LUE_{chl} = \frac{GPP}{fAPAR_{chl} \times PAR}$) for $fAPAR_{chl}$. Table 1 shows average LUE_{chl} (maize, 0.70; soybean, 0.45 g C mol⁻¹ Photosynthetic Photon Flux Density (PPFD)) is greater than LUE_{canopy} (maize, 0.58; soybean, 0.35 g C mol⁻¹ PPFD) for both crop types in each field. Neither the average LUE_{canopy} nor the average LUE_{chl} changed much from field to field per crop type. The functions were employed to estimate GPP. The improvement achieved by replacing MOD15A2 FPAR with $fAPAR_{chl}$ to estimate crop GPP is obvious in terms of R^2 and RMSE for each crop type in each field. The performance of $fAPAR_{chl}$ in the irrigated field (US-NE2) is better than in the rainfed field (US-NE3) for both maize and soybean, as expressed in terms of R^2 and RMSE.

We combined data for maize from all three fields and combined data for soybean from US-NE2 and US-NE3 to determine more general relationships for both crop types using MOD15A2 FPAR and $fAPAR_{chl}$ to simulate GPP. Tower-based mean daily GPP values during the growing season were 12.44 and 8.07 g C m⁻² d⁻¹ for maize and soybean, respectively. Fig. 2 shows the comparison of simulated GPP using MOD15A2 FPAR and $fAPAR_{chl}$ against tower flux GPP for maize and soybean, respectively. The GPP estimation performance using $fAPAR_{chl}$ is noticeably better than using MOD15A2 FPAR for both crop types: for maize, R^2 increases from 0.68 to 0.87 and RMSE decreases from 4.59 to 2.88 g C m⁻² d⁻¹; for soybean, R^2 increases from 0.46 to 0.83 and RMSE decreases from 3.72 to 2.10 g C m⁻² d⁻¹.

4. Discussion

Table 1 shows average LUE_{chl} of maize (0.70 g C mol⁻¹ PPFD) is much higher than average LUE_{chl} of soybean (0.45 g C mol⁻¹ PPFD). The MOD17A2 GPP algorithm and product assume that the maximum LUE for crop is 0.68 g C/MJ (≈ 0.15 g C mol⁻¹ PPFD) in the Biome Properties Look-Up Table (BPLUT) (Running et al., 2004; Zhao & Running, 2010; Zhao, Running, & Nemani, 2006) which is significantly lower than the mean LUE_{chl} values for both maize (C4 type) and soybean (C3 type) in the study fields. This result demonstrates that, in order to achieve better GPP estimates, the MOD17A2 GPP algorithm should expand the BPLUT by splitting the single “crop” type into multiple crop types with updated maximum LUEs. Potential approaches for estimating daily LUE_{chl} include the photochemical reflectance index (PRI) retrieved from MODIS ocean bands or from other sensors (Hilker et al., 2008, 2010; Zhang et al., in review).

Phenology indicated by MOD15A2 FPAR incorrectly describes an earlier start of growing season than was indicated by tower flux GPP, field $fAPAR_{canopy}$ or $fAPAR_{green}$ (Fig. 1(a)). MOD15A2 FPAR reached ~ 0.3 in late April and early May even though the new crop leaves had not yet appeared. The midsummer MOD15A2 FPAR was lower than field $fAPAR_{canopy}$ (Fig. 1(a)). The difference between field $fAPAR_{green}$ and retrieved $fAPAR_{chl}$ during mid July to early August was ~ 0.21 . Earlier

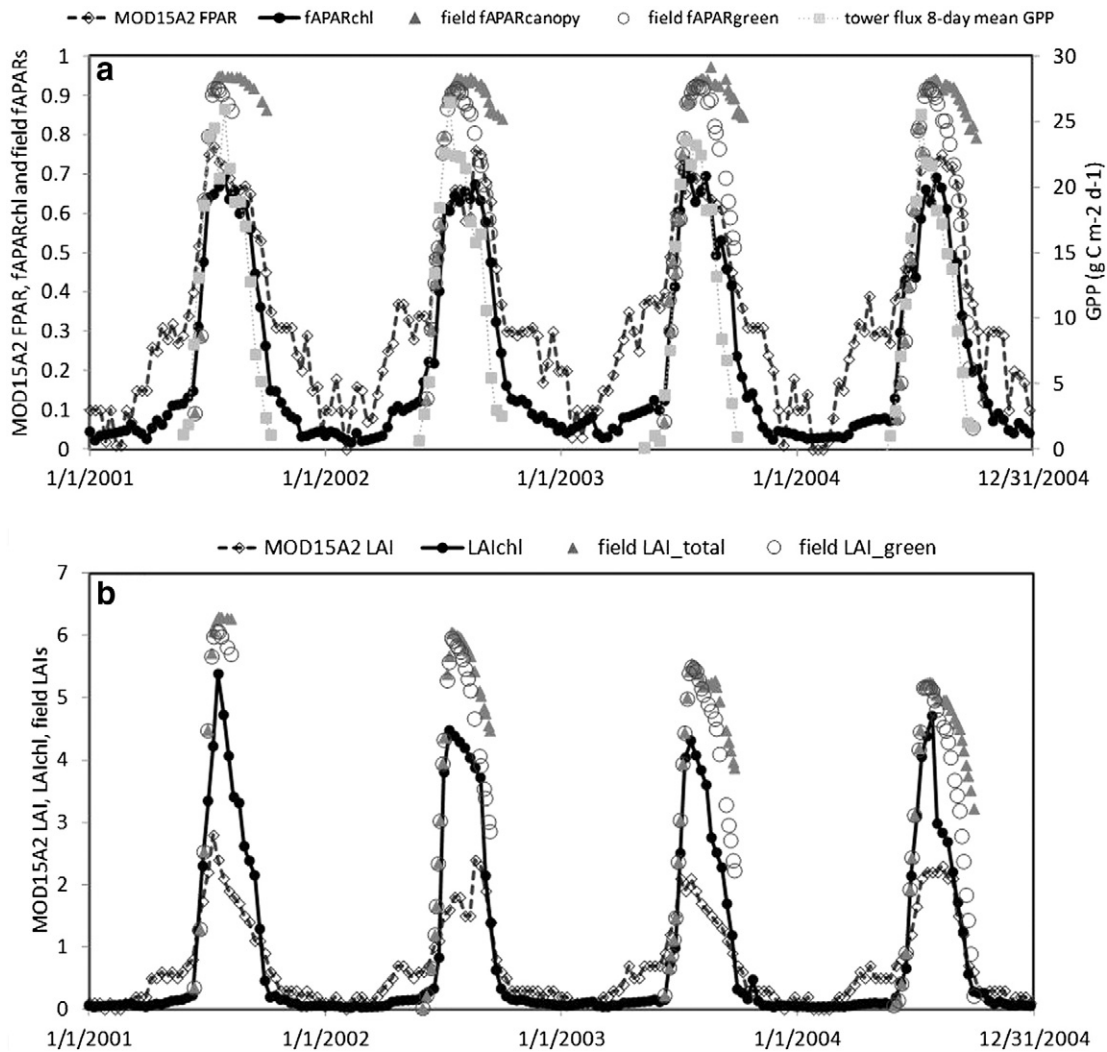


Fig. 1. The seasonal dynamics at US-NE1 during 2001–2004 for: (a) MOD15A2 FPAR, $fAPAR_{chl}$, field $fAPAR_{canopy}$, field $fAPAR_{green}$, and the tower flux 8-day mean daily GPP; and (b) MOD15A2 LAI, retrieved LAI_{chl} , field LAI_{total} and field LAI_{green} .

studies have reported the proportion of PAR absorbed by non-photosynthetic components of a mature green leaf ranged from 15% to 20% of the PAR absorbed by the whole leaf (Evans, 1987; von Caemmerer, 2000). Leaf dry matter in the leaf tissue is increasing after

Table 1

List of regression linear functions between tower flux GPP and APAR: $y = ax$ (y is tower GPP, $APAR = [MOD15A2\ FPAR] \times PAR$ or $APAR = fAPAR_{chl} \times PAR$). Slope (“ a ”) means average light use efficiency (LUE, $g\ C\ mol^{-1}\ PPF$) at canopy level or at chlorophyll level, respectively. R^2 and RMSE ($g\ C\ m^{-2}\ d^{-1}$) also are reported.

| | | $y = ax$ | $y = ax$ |
|---------------------|-------|----------------------------------|------------------------------|
| | | $x = [MOD15A2\ FPAR] \times PAR$ | $x = fAPAR_{chl} \times PAR$ |
| US-NE1 (maize) | R^2 | $y = 0.58x$ 0.66 | $y = 0.71x$ 0.86 |
| | RMSE | 4.87 | 2.88 |
| US-NE2 (maize) | R^2 | $y = 0.61x$ 0.72 | $y = 0.69x$ 0.94 |
| | RMSE | 4.43 | 2.06 |
| US-NE2 (soybean) | R^2 | $y = 0.37x$ 0.46 | $y = 0.45x$ 0.88 |
| | RMSE | 3.80 | 1.81 |
| US-NE3 (maize) | R^2 | $y = 0.54x$ 0.67 | $y = 0.70x$ 0.85 |
| | RMSE | 4.31 | 2.93 |
| US-NE3 (soybean) | R^2 | $y = 0.33x$ 0.48 | $y = 0.44x$ 0.74 |
| | RMSE | 3.61 | 2.49 |

early crop growth (Demarez et al., 1999; Gond, de Pury, Veroustraete, & Ceulemans, 1999; Smart & Bingham, 1974) which partly accounts for the difference between $fAPAR_{chl}$ retrievals and field $fAPAR_{green}$ values in late July, August and September. The computing of field $fAPAR_{green}$ does not consider the impact of litter components and non-photosynthetic pigments within “green leaves” which also contributes the difference between $fAPAR_{chl}$ and field $fAPAR_{green}$. The field measured $fAPAR_{canopy}$ is composed of $fAPAR_{foliage}$ and $fAPAR_{stem}$ (by corn stalks and other non-foliar components). Therefore, $fAPAR_{green}$ calculated with Eq. (1) might be greater than actual $fAPAR$ by green leaves. All these factors might also account for the difference between field LAI_{green} and retrieved LAI_{chl} in late July, August and September.

The $fAPAR_{chl}$ and LAI_{chl} retrieval algorithm (Zhang et al., 2013) includes search ranges for soil/background reflectance and stem reflectance for MODIS bands 1–7 as input, and does not need biome type as input for inversion, and can successfully invert leaf chlorophyll content, leaf dry matter, leaf water content and leaf non-photosynthetic pigment using PROSAIL2 and surface reflectance of MODIS bands 1–7. When there are no leaves standing in the field, whether live leaves or dead leaves, the retrieved $fAPAR_{chl}$ and LAI_{chl} will be \sim zero. In contrast, the MOD15A2 LAI/FPAR algorithm needs biome type of each pixel as input for inversion and does not intend to achieve $fAPAR_{foliage}$, $fAPAR_{chl}$ or $fAPAR_{non-chl}$. Upstream activities of the MOD15A2 LAI/FPAR and MODIS $fAPAR_{chl}$ retrieval processes include L1B data calibration, gridding and atmospheric correction. Both the differences among the

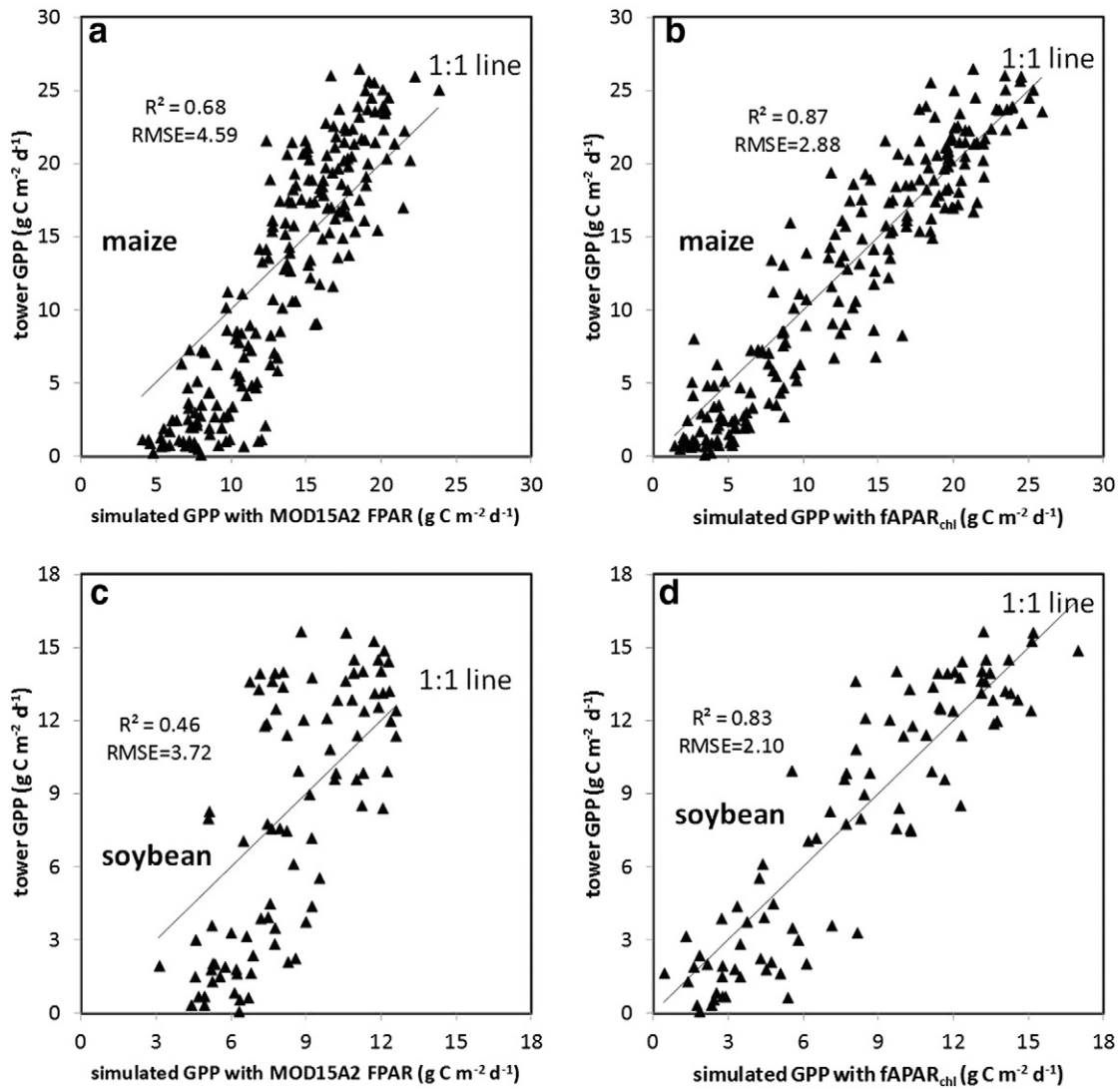


Fig. 2. Comparison of simulated GPP with tower flux GPP: (a) GPP was simulated using MOD15A2 FPAR for all three maize fields; (b) GPP was simulated using $fAPAR_{chl}$ for all three maize fields; (c) GPP was simulated using MOD15A2 FPAR for soybean in US-NE2 and US-NE3; and (d) GPP was simulated using $fAPAR_{chl}$ for soybean in US-NE2 and US-NE3.

upstream activities and the differences among the MOD15A2 LAI/FPAR and the $LAI_{chl}/fAPAR_{chl}$ retrieval algorithms might contribute to the performance difference of the MOD15A2 LAI/FPAR product and the $LAI_{chl}/fAPAR_{chl}$ product.

5. Conclusion

For these study fields, MOD15A2 FPAR overestimated field $fAPAR_{canopy}$ in spring and fall, and underestimated the peak field $fAPAR_{canopy}$ values in summer. MOD15A2 LAI also overestimated field LAI in spring, and underestimated field total LAI in summer. This suggests that the slope “a” in Table 1 for MOD15A2 FPAR would differ from field LUE_{canopy} ($field\ LUE_{canopy} = \frac{GPP}{[field\ fAPAR_{canopy}] + PAR}$) because the product $[MOD15A2\ FPAR] \times PAR$ overestimated field $fAPAR_{canopy}$ in spring and fall, and underestimated it in summer. The eye ball inspection approach of “green leaves” (Gitelson et al., 2012; Peng et al., 2011, 2013; Viña & Gitelson, 2005; Viña, Gitelson, Nguy-Robertson, & Peng, 2011) does not tell how much non-photosynthetic pigment and dry matter exists, especially during the middle and late growing season. This can limit the use of $fAPAR_{green}$ and LAI_{green} in GPP estimation.

GPP simulated with $fAPAR_{chl}$ was corroborated with tower flux GPP in crops. Replacing MOD15A2 FPAR with $fAPAR_{chl}$ resulted in improvement and reduction of uncertainties of crop GPP estimates. Overall, for maize,

R^2 increased by ~ 0.19 and RMSE decreased by $1.71\ g\ C\ m^{-2}\ d^{-1}$; for soybean, R^2 increased by ~ 0.37 and RMSE decreased by $1.62\ g\ C\ m^{-2}\ d^{-1}$. Investigations on GPP estimation performance with $fAPAR_{chl}$ versus MOD15A2 FPAR for other plant functional types are needed. GPP estimated with MODIS $fAPAR_{chl}$ over the Bartlett Experimental Forest in New Hampshire also was validated with its tower GPP (Cheng, Zhang, Lyapustin, Wang, & Middleton, 2014). The MODIS $fAPAR_{chl}$ and LAI_{chl} products, compared to MOD15A2 LAI/FPAR, have the potential to improve the parameterization of absorbed PAR for vegetation photosynthesis in satellite-based GPP monitoring algorithms (e.g., the MOD17A2 GPP algorithm) (Cheng et al., 2014), land surface models and terrestrial carbon cycle models.

Acknowledgments

This study was supported by NASA Terrestrial Ecology project (Grant No., NNX12AJ51G; PI, Q. Zhang) and NASA Science of Terra and Aqua project (Grant No., NNX14AK50G; PI, Q. Zhang) (Dr. Diane Wickland, manager). We would like to thank the support and the use of facilities and equipment provided by the Center for Advanced Land Management Information Technologies and the Carbon Sequestration program, University of Nebraska—Lincoln. Site-specific climate and CO_2 flux data are distributed by AmeriFlux network (<http://public.ornl.gov/>)

ameriflux), supported by Carbon Dioxide Information Analysis Center at the Oak Ridge National Laboratory of the Department of Energy. We are grateful to Drs. Anatoly Gitelson and Yi Peng for helpful discussion and comments and for providing field fAPAR_{canopy}, fAPAR_{green}, LAI and LAI_{green}. USDA is an equal opportunity provider and employer.

References

- Cheng, Y., Zhang, Q., Lyapustin, A. I., Wang, Y., & Middleton, E. M. (2014). Impacts of light use efficiency and fPAR parameterization on gross primary production modeling. *Agricultural and Forest Meteorology*, 189–190, 187–197.
- Deering, D. W. (1978). *Rangeland reflectance characteristics measured by aircraft and space-craft sensors*. College Station, TX: Texas A&M University, 338.
- Demarez, V., Gastellu-Etchegorry, J. P., Mougou, E., Marty, G., Proisy, C., Dufrene, E., et al. (1999). Seasonal variation of leaf chlorophyll content of a temperate forest. Inversion of the PROSPECT model. *International Journal of Remote Sensing*, 20, 879–894.
- Emmanuel, W. R., Killough, G. G., Post, W. M., & Shugart, H. H. (1984). Modelling terrestrial ecosystems in the global carbon cycle with shifts in carbon storage capacity by land-use change. *Ecology*, 65, 970–983.
- Evans, J. R. (1987). The dependence of quantum yield on wavelength and growth irradiance. *Australian Journal of Plant Physiology*, 14, 69–79.
- Gelman, A., Carlin, J. B., Stern, H. S., & Rubin, D. B. (2000). Markov chain simulation. In A. Gelman, J. B. Carlin, H. S. Stern, & D. B. Rubin (Eds.), *Bayesian data analysis*. New York: Chapman & Hall/CRC.
- Gitelson, A. A., Peng, Y., Masek, J. G., Rundquist, D. C., Verma, S., Suyker, A., et al. (2012). Remote estimation of crop gross primary production with Landsat data. *Remote Sensing of Environment*, 121, 404–414.
- Gitelson, A. A., Verma, S. B., Vina, A., Rundquist, D. C., Keydan, G., Leavitt, B., et al. (2003). Novel technique for remote estimation of CO₂ flux in maize. *Geophysical Research Letters*, 30, 1486.
- Gitelson, A. A., Viña, A., J. G. M., Verma, S. B., & Suyker, A. E. (2008). Synoptic monitoring of gross primary productivity of maize using Landsat data. *IEEE Geoscience and Remote Sensing Letters*, 5, 133–137.
- Gond, V., de Pury, D. G. G., Veroustraete, F., & Ceulemans, R. (1999). Seasonal variations in leaf area index, leaf chlorophyll, and water content; scaling-up to estimate fAPAR and carbon balance in a multilayer, multispecies temperate forest. *Tree Physiology*, 19, 673–679.
- Guindin-García, N., Gitelson, A. A., Arkebauer, T. J., Shanahan, J., & Weiss, A. (2012). An evaluation of MODIS 8- and 16-day composite products for monitoring maize green leaf area index. *Agricultural and Forest Meteorology*, 161, 15–25.
- Hilker, T., Coops, N. C., Schwalm, C. R., Jassal, R. S., Black, T. A., & Krishnan, P. (2008). Effects of mutual shading of tree crowns on prediction of photosynthetic light-use efficiency in a coastal Douglas-fir forest. *Tree Physiology*, 28, 825–834.
- Hilker, T., Hall, F. G., Coops, N. C., Lyapustin, A., Wang, Y., Nesic, Z., et al. (2010). Remote sensing of photosynthetic light-use efficiency across two forested biomes: spatial scaling. *Remote Sensing of Environment*, 114, 2863–2874.
- Justice, C. O., Vermote, E., Townshend, J. R. G., Defries, R., Roy, D. P., Hall, D. K., et al. (1998). The Moderate Resolution Imaging Spectroradiometer (MODIS): land remote sensing for global change research. *IEEE Transactions on Geoscience and Remote Sensing*, 36, 1228–1249.
- Knyazikhin, Y., Martonchik, J. V., Myneni, R. B., Diner, D. J., & Running, S. W. (1998). Synergistic algorithm for estimating vegetation canopy leaf area index and fraction of absorbed photosynthetically active radiation from MODIS and MISR data. *Journal of Geophysical Research*, 103, 32257–32275.
- Lyapustin, A., Martonchik, J., Wang, Y., Laszlo, I., & Korkin, S. (2011). Multi-Angle Implementation of Atmospheric Correction (MAIAC): Part 1. Radiative transfer basis and look-up tables. *Journal of Geophysical Research*, 116, D03210.
- Lyapustin, A., Wang, Y., & Frey, R. (2008). An automatic cloud mask algorithm based on time series of MODIS measurements. *Journal of Geophysical Research*, 113.
- Lyapustin, A., Wang, Y., Laszlo, I., Hilker, T., Hall, F., Sellers, P., et al. (2012). Multi-Angle Implementation of Atmospheric Correction for MODIS (MAIAC). 3: atmospheric correction. *Remote Sensing of Environment*, 127, 385–393.
- Lyapustin, A., Wang, Y., Laszlo, I., Kahn, R., Korkin, S., Remer, L., et al. (2011). Multi-Angle Implementation of Atmospheric Correction (MAIAC): Part 2. Aerosol algorithm. *Journal of Geophysical Research*, 116, D03211.
- Metropolis, N., Rosenbluth, A. W., Rosenbluth, M. N., Teller, A. H., & Teller, E. (1953). Equations of state calculations by fast computing machines. *Journal of Chemical Physics*, 21, 1087–1092.
- Monteith, J. L. (1972). Solar-radiation and productivity in tropical ecosystems. *Journal of Applied Ecology*, 9, 747–766.
- Monteith, J. L. (1977). Climate and efficiency of crop production in Britain. *Philosophical Transaction of the Royal Society of London B: Biological Sciences*, 281, 277–294.
- Myneni, R. B., Hoffman, S., Knyazikhin, Y., Privette, J. L., Glassy, J., Tian, Y., et al. (2002). Global products of vegetation leaf area and fraction absorbed PAR from year one of MODIS data. *Remote Sensing of Environment*, 83, 214–231.
- Myneni, R. B., Nemani, R. R., & Running, S. W. (1997). Estimation of global leaf area index and absorbed PAR using radiative transfer models. *IEEE Transactions on Geoscience and Remote Sensing*, 35, 1380–1393.
- Peng, Y., Gitelson, A. A., Keydan, G. P., Rundquist, D. C., & Moses, W. J. (2011). Remote estimation of gross primary production in maize and support for a new paradigm based on total crop chlorophyll content. *Remote Sensing of Environment*, 115, 978–989.
- Peng, Y., Gitelson, A. A., & Sakamoto, T. (2013). Remote estimation of gross primary productivity in crops using MODIS 250 m data. *Remote Sensing of Environment*, 128, 186–196.
- Running, S. W. (1984). Microclimate control of forest productivity: analysis by computer simulation of annual photosynthesis/transpiration balance in different environment. *Agricultural and Forest Meteorology*, 32, 267–288.
- Running, S. W., & Coughlan, J. C. (1988). A general-model of forest ecosystem processes for regional applications. I. Hydrologic balance, canopy gas-exchange and primary production processes. *Ecological Modelling*, 42, 125–154.
- Running, S. W., & Gower, S. T. (1991). Forest-BGC, a general-model of forest ecosystem processes for regional applications. II. Dynamic carbon allocation and nitrogen budgets. *Tree Physiology*, 9, 147–160.
- Running, S., Nemani, R., Heinsch, F., Zhao, M., Reeves, M., & Hashimoto, H. (2004). A continuous satellite-derived measure of global terrestrial primary production. *Bioscience*, 54, 547–560.
- Running, S. W., Thornton, P. E., Nemani, R., & Glassy, J. M. (2000). Global terrestrial gross and net primary productivity from the Earth Observing System. In O. E. Sala, R. B. Jackson, H. A. Mooney, & R. W. Howarth (Eds.), *Methods in ecosystem science* (pp. 44–57). New York: Springer Verlag.
- Sellers, P. J. (1985). Canopy reflectance, photosynthesis and transpiration. *International Journal of Remote Sensing*, 6, 1335–1372.
- Sellers, P. (1987). Canopy reflectance, photosynthesis and transpiration. II. The role of biophysics in the linearity of their interdependence. *Remote Sensing of Environment*, 21, 143–183.
- Smart, R. E., & Bingham, G. E. (1974). Rapid estimates of relative water content. *Plant Physiology*, 53, 258–260.
- Suyker, A. E., Verma, S. B., Burba, G. G., & Arkebauer, T. J. (2005). Gross primary production and ecosystem respiration of irrigated maize and irrigated soybean during a growing season. *Agricultural and Forest Meteorology*, 131, 180–190.
- Tucker, C. J. (1979). Red and photographic infrared linear combinations for monitoring vegetation. *Remote Sensing of Environment*, 8, 127–150.
- Ustin, S. L., Wessman, C. A., Curtiss, B., Kasischke, E., Way, J., & Vanderbilt, V. C. (1991). Opportunities for using the EOS Imaging Spectrometers and synthetic aperture radar in ecological models. *Ecology*, 72, 1934–1945.
- Viña, A., & Gitelson, A. A. (2005). New developments in the remote estimation of the fraction of absorbed photosynthetically active radiation in crops. *Geophysical Research Letters*, 32.
- Viña, A., Gitelson, A. A., Nguy-Robertson, A. L., & Peng, Y. (2011). Comparison of different vegetation indices for the remote assessment of green leaf area index of crops. *Remote Sensing of Environment*, 115, 3468–3478.
- von Caemmerer, S. (2000). *Biochemical models of leaf photosynthesis*. Collingwood, Vic., Australia: CSIRO.
- Wolfe, R., Roy, D., & Vermote, E. (1998). The MODIS land data storage, gridding and compositing methodology: Level 2 Grid. *IEEE Transactions on Geosciences and Remote Sensing*, 36, 1324–1338.
- Zhang, Q. (2003). *Improving estimation of terrestrial gross primary productivity (GPP): retrieval of fraction of photosynthetically active radiation absorbed by chlorophyll (fAPARchl) versus fAPAR*. NASA Earth System Science (ESS) Fellowship Program.
- Zhang, Q., Cheng, Y.-B., Lyapustin, A. I., Wang, Y., Xiao, X., Suyker, A., et al. (2014). Estimation of crop gross primary production (GPP): I. Impact of MODIS observation footprint area and impact of vegetation BRDF characteristics. *Agricultural and Forest Meteorology*, 191, 51–63.
- Zhang, Q., Cheng, Y.-B., Lyapustin, A. I., Wang, Y., Zhang, X., Suyker, A., et al. (2014). Estimation of crop gross primary production (GPP): II. Do the scaled vegetation indices improve performance? *Agricultural and Forest Meteorology* (in revision).
- Zhang, Q., Middleton, E. M., Cheng, Y.-B., Huemmrich, K. F., Cook, B. D., Corp, L. A., et al. (2014w). Remote estimation of corn daily gross primary production (GPP): integration of fAPAR_{chl} and PRI. *Agricultural and Forest Meteorology* (in review).
- Zhang, Q., Middleton, E. M., Cheng, Y.-B., & Landis, D. R. (2013). Variations of foliage chlorophyll fAPAR and foliage non-chlorophyll fAPAR (fAPAR_{chl}, fAPAR_{non-chl}) at the Harvard Forest. *IEEE Journal of Selected Topics in Applied Earth Observations and Remote Sensing*, 6, 2254–2264.
- Zhang, Q., Middleton, E. M., Gao, B.-C., & Cheng, Y.-B. (2012). Using EO-1 hyperion to simulate HySpIRI products for a coniferous forest: the fraction of PAR absorbed by chlorophyll (fAPARchl) and leaf water content (LWC). *IEEE Transactions on Geoscience and Remote Sensing*, 50, 1844–1852.
- Zhang, Q., Middleton, E. M., Margolis, H. A., Drolet, G. G., Barr, A. A., & Black, T. A. (2009). Can a satellite-derived estimate of the fraction of PAR absorbed by chlorophyll (fAPARchl) improve predictions of light-use efficiency and ecosystem photosynthesis for a boreal aspen forest? *Remote Sensing of Environment*, 113, 880–888.
- Zhang, Q., Xiao, X. M., Braswell, B., Linder, E., Baret, F., & Moore, B. (2005). Estimating light absorption by chlorophyll, leaf and canopy in a deciduous broadleaf forest using MODIS data and a radiative transfer model. *Remote Sensing of Environment*, 99, 357–371.
- Zhao, M., & Running, S. (2010). Drought-induced reduction in global terrestrial net primary production from 2000 through 2009. *Science*, 329, 940–943.
- Zhao, M., Running, S., & Nemani, R. R. (2006). Sensitivity of Moderate Resolution Imaging Spectroradiometer (MODIS) terrestrial primary production to the accuracy of meteorological reanalyses. *Journal of Geophysical Research*, 111, G01002.